SLM-Based Mode Division Multiplexing System With 6×6 Sparse Equalization

Kai Shi, *Member, IEEE*, Feng Feng, George S. D. Gordon, Timothy D. Wilkinson, and Benn C. Thomsen, *Member, IEEE*

***Abstract*— We demonstrate a mode division multiplexing (MDM) system over an 8 km conventional graded index multimode fiber. Spatial light modulators (SLMs) are used to multiplex and demultiplex three linearly polarized (LP) modes (LP01, LP11a, and LP11b) in two polarizations. A 6 × 6 sparse frequency domain equalizer (FDE) is used as the channel impulse response of the SLM-based MDM system is found to be sparse due to the large crosstalk at the mode MUX/DEMUX and small coupling in the fiber. The signal transmitted on each mode is recovered with improved performance over conventional FDEs. The results indicate that this system can be used in short reach transmission applications to increase the system capacity.**

***Index Terms*— Mode division multiplexing, sparse equalizer, spatial light modulator.**

I. Introduction

THE communication bandwidth requirements of datacenters and high performance computing (HPC) systems have been growing enormously. These networks require short distance network connectivity with high bandwidth and low power consumption [1]. To date, multimode fibers (MMFs) have been widely deployed in these systems as they offer efficient coupling from light sources and low-cost splices and connectors between fibers [2]. In order to meet the requirements of high bandwidth and low density, mode division multiplexing (MDM), which has attracted significant research interest for long haul transmission [3]–[5], can also be used to meet the required capacity growth of datacenters and HPC systems.

Recently, mode-multiplexed transmission over conventional graded index multimode fiber (GI-MMF) has been achieved by using high performance mode selective photonic lanterns, where the multiplexed modes are fixed for a given index profile design of the photonic lanterns [6]. Using spatial light modulator (SLM) based reconfigurable mode MUX/DEMUX, the spatial and polarization modes in a prototype few mode fiber (FMF) can be selectively launched and received, which can significantly reduce the multiple-input multiple-output (MIMO) digital signal processing (DSP) complexity for short distance transmission [7]. This is due to the large difference in phase velocities between the modes in the GI-MMF that prevents the mode from coupling while propagating along the fiber. However, the number of supported modes of the system is limited by the size of the SLM, as each mode is multiplexed/demultiplexed at different areas of the SLM [8]. With superposition of the phase masks for each fiber mode, the number of modes in a GI-MMF can be scaled [9]. However, in previous works, the SLM-based mode MUX for the transmission experiments over conventional GI-MMF has been limited to launching the channels into two modes: LP01 and an arbitrary higher order mode [10]. In addition, despite the use of a selective SLM-based MUX/DEMUX, MIMO DSP remains necessary for such systems, as the modal selectivity when launching into a conventional multimode fiber is only around 8∼10 dB. As a contrast, due to the difference in phase velocities of the modes, which results in a large differential mode delay (DMD) in the fiber (0.36 ns/km for the LP11 mode, 0.61 ns/km for the LP02 and LP21 modes), the coupling between the mode groups in the 8 km GI-MMF is found to be less than −20 dB. As a result of the modal mixing predominately occurring at the MUX and DEMUX, the impulse response of the complete MIMO channel (MUX, transmission fiber and DEMUX) is sparse. Therefore, sparse frequency domain equalizers (FDEs) can be used to achieve relatively low DSP complexity and improve the system performance compared with conventional uniformly spaced tap-delay-line MIMO equalizers [11].

In this letter, as an extension of our previous work in [11] that multiplexes 2 channels using 2 mode groups, we demonstrate a 6×6 MDM system over an 8 km conventional GI-MMF using an SLM-based MUX/DEMUX that uses sparse equalization. The fiber is an OM2 fiber with a core diameter of 50 μm and a refractive index difference of 1 %. The fiber loss is $\leq$ 0.6 dB/km at 1300 nm and the macro bending loss is $\leq$0.5 dB with 2 turns on a mandrel with a radius of 7.5 mm. Two polarizations of three linearly polarized (LP) modes in the GI-MMF (LP01, LP11a and LP11b), each of which is modulated with a 28 Gbaud quadrature phase shift keying (QPSK) signal, are selectively launched and detected using SLM-based mode MUX/DEMUX. The channel impulse response shows a strong crosstalk (∼−12 dB) at the mode MUX/DEMUX as a result of optical aberrations in the launch system. The resultant sparse channel is then equalized using an improved

Manuscript received March 20, 2015; revised May 9, 2015; accepted May 13, 2015. Date of publication May 21, 2015; date of current version July 10, 2015. This work was supported by the U.K. Engineering and Physical Sciences Research Council under Grant EP/J008842/1.

K. Shi and B. C. Thomsen are with the Department of Electronic and Electrical Engineering, University College London, London WC1E 7JE, U.K. (e-mail: k.shi@ucl.ac.uk; b.thomsen@ucl.ac.uk).

F. Feng, G. S. D. Gordon, and T. D. Wilkinson are with the Department of Engineering, University of Cambridge, Cambridge CB3 0FA, U.K. (e-mail: ff263@cam.ac.uk; gsdg2@cam.ac.uk; tdw13@cam.ac.uk).

Color versions of one or more of the figures in this letter are available online at http://ieeexplore.ieee.org.

Digital Object Identifier 10.1109/LPT.2015.2436067

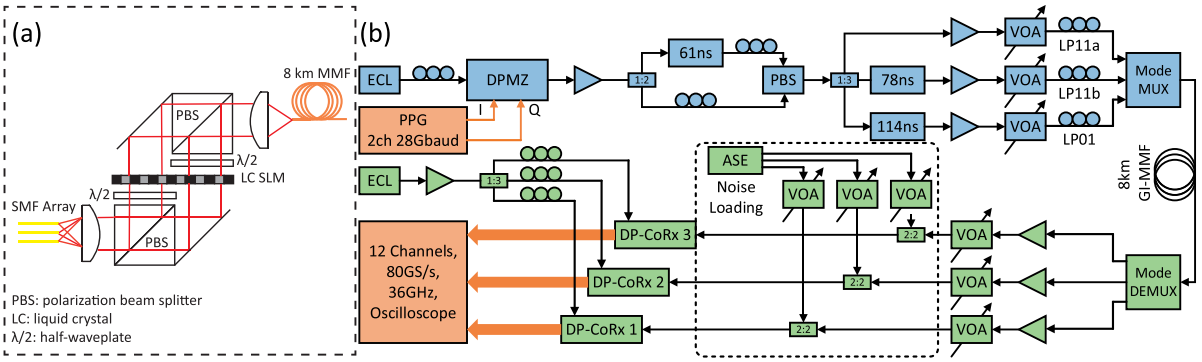

Fig. 1. (a) SLM-based mode MUX/DEMUX. (b) Experimental setup. ECL: external cavity laser, PPG: pulse pattern generator, DPMZ: dual parallel Mach-Zehnder modulator, VOA: variable optical attenuator, ASE: Amplified spontaneous emission noise, DP-CoRx: dual polarization coherent receiver.

proportionate normalized least-mean-square (IPNLMS) FDE. An improvement of the system performance of 0.2 dB is achieved over the conventional FDE.

II. SLM-Based Mode MUX/DEMUX

Fig. 1 (a) illustrates the configuration of the SLM-based mode MUX/DEMUX used at each end of the 8 km GI-MMF. The input polarization state is first split into two orthogonal polarizations each of which is then aligned with the required polarization of the SLM using half-waveplates. The SLM area is divided into two, with each half processing one polarization independently of the other. Having passed through the SLM, the two orthogonal polarizations are recombined. Each optical channel is then considered a mapping between a single fiber and polarization state in the MUX SMF array and a fiber and polarization state in the DEMUX SMF array. The mode transfer matrices of each of these optical channels can be characterized by launching each mode in each polarization one at a time at MUX and analyzing the modal content of the output beam at the DEMUX [9]. Fig. 2 (a) shows the measured mode transfer matrix of the channel using the most central SMF of the MUX input fiber array and similarly for the DEMUX array. Fig. 2 (b) shows the measured mode transfer matrix of a channel using an offset SMF at the MUX. It can be seen that there is significantly more modal crosstalk than Fig. 2 (a). This is because the offset SMF introduces optical distortions that cannot be fully corrected using multiplicative Zernike phase masks. Currently, this system is only able to compensate aberrations using Zernike phase masks and so optical distortion is the main source of modal crosstalk at the MUX and DEMUX.

When operating as a mode multiplexer, Gaussian beams from each fiber in the SMF array (spaced 250 μm apart) illuminate the SLM. The SLM then displays a superposition of mode phase masks such that each illumination source will project the desired mode or combination of modes for that channel onto the MMF facet. Within this superposition the phase masks for each channel are weighted with complex coefficients, which are determined through an iterative feedback algorithm so as to equalize power and minimize crosstalk between channels. Because the SLMs are phase-only devices, the superposition of the phase masks discards

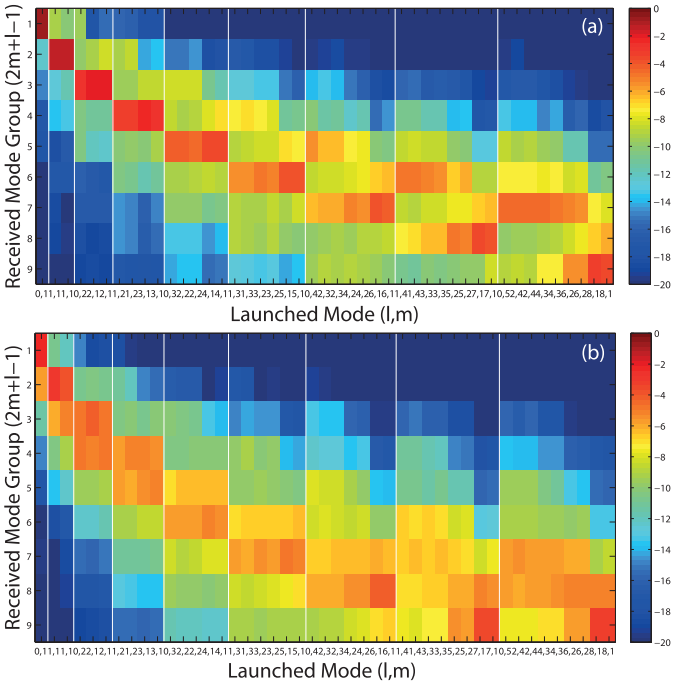

Fig. 2. (a) Mode transfer matrix of the channel using the central SMF at the MUX/DEMUX. (b) Mode transfer matrix of the channel with an offset SMF at the MUX/DEMUX.

amplitude information. This results in a power loss equivalent to that of a traditional phase mask and beam splitter approach. This may also introduce a small amount of additional crosstalk (<20 dB) but in this case the MUX/DEMUX crosstalk is dominated by optical distortions, as can be seen from the mode-transfer matrices that do not rely on superposition. As we can see from Fig. 2 (a) that the worst case gives a crosstalk of approximately −10 dB between the first three mode groups, which has a similar level of crosstalk (−10.5 dB, 40 km) comparing with the mode MUX/DEMUX using separated phase masks for each mode [7].

III. MDM System

The diagram of the MDM system is shown in Fig. 1 (b), where standard 28 Gbaud QPSK transmitters and receivers are used for the 6×6 MDM system. The in-phase (I) and

quadrature (Q) component of the QPSK signal are generated using the two data outputs of a pulse pattern generator (PPG) to drive a dual parallel Mach-Zehnder (DPMZ) modulator. Each output is a 28 Gbit/s data signal, which is derived from two interleaved 14 Gbit/s pseudo random binary sequence (PRBS) of length $2^{15} - 1$. The signals that are modulated on the two polarizations of each LP mode are decorrelated with a relative delay of 61 ns (1714 symbols). The polarization multiplexed signals are then separated into three tributaries, each of which is again decorrelated with a relative delay of 0 ns, 78 ns (2190 symbols) and 114 ns (3182 symbols) respectively. As shown in Fig. 1 (b), the three decorrelated signals are selectively launched into the LP11a, LP11b and LP01 modes of the 8 km GI-MMF by using the SLM mode MUX as described in section II. At the mode DEMUX, the signals from each spatial channel in the MMF are routed to different ports of the output fiber array. This is achieved by displaying on the SLM a superposition of the phase masks for each channel, each with a different phase tilt. The central SMF of the fiber array is used for launching and receiving the LP01 mode, while the offset SMFs of the fiber array are used for the LP11a/b modes. Afterwards, amplified spontaneous emission (ASE) noise is combined with the demultiplexed signal to vary the received optical signal to noise ratio (OSNR). The noise loaded signal is then detected by three integrated coherent receivers and a 12-channel real time oscilloscope, where the signals are sampled at 80 GSample/s before offline MIMO DSP to recover the data.

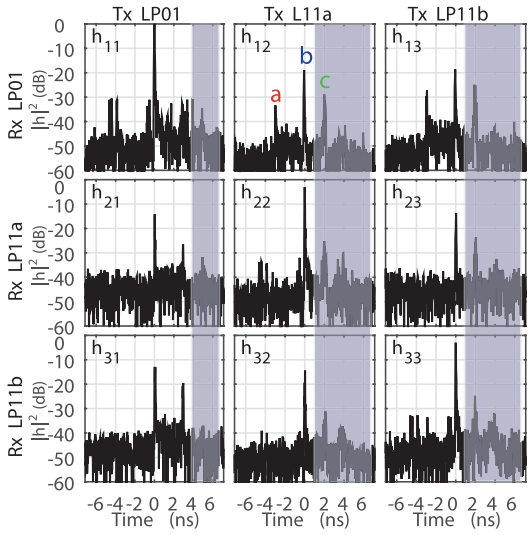

Fig. 3. The estimated channel impulse response $h_{i,j}$ after 8 km of GI-MMF. Impulses in the shaded area are the signals that coupled into modes with higher mode indices than the selected modes at the MUX and then coupled back into the selected modes at the DMUX.

TABLE I
CROSSTALK AND COUPLING

Crosstalk at MUX/DEMUX (dB)				Coupling in the fiber (dB)			
Rx \Tx	LP01	LP11a	LP11b	Rx \Tx	LP01	LP11a	LP11b
LP01	\	-14.9	-13.8	LP01	\	-28.2	-23.7
LP11a	-13.7	\	-10.1	LP11a	-22.3	\	
LP11b	-9.2	-12.7	\	LP11b	-21.9		\

A. Channel Impulse Response

To estimate the channel impulse response from the received data signals, the constant-modulus algorithm (CMA) is used in the equalizer to undo the crosstalk of the spatial channels after the compensation of the impairments of the coherent front-ends. This is followed by the carrier phase estimation and correction using the Viterbi-Viterbi algorithm. After a decision is made for each symbol of the recovered channel, the bit error rate (BER) is calculated. The recovered data sequence is then upsampled to two samples per symbol to recreate the unknown transmitted data signal (QPSK). This reconstructed signal along with the received signal is subsequently used for the least squares (LS) estimation of the channel impulse response [11]. We use a LS channel estimation rather than simply inverting the response obtained from the CMA equalizer as this approach is more robust. The resulting channel impulse response is plotted in Fig. 3, where the coefficients of the two polarizations of each mode are averaged.

The large central impulses in the diagonal matrices represent the ideal channel response, where the energy is preserved in the selectively launched mode. The other sparse impulses in the channel response arise from the crosstalk that occurs either in the mode MUX or DEMUX. For example, impulse (b) in h12 represents the crosstalk from the LP11a mode to the LP01 mode at the mode DEMUX as it propagates at the same speed as the central impulse in h22. However, the impulse (a) in h12 represents the crosstalk from the LP11a mode to the LP01 mode at the mode MUX which propagates faster than the central impulse in h22. The impulse (c) in h12 indicates coupling from the LP11a mode to the next higher order mode group (LP02, LP12a or LP12b) at the mode MUX, which is then coupled back into the LP01 mode at the mode DEMUX. It can be noticed that the magnitude of the channel coefficients in between the sparse impulses are approximately 40 dB lower than the central impulses, which shows that the coupling between the modes within the transmission fiber is much weaker than that occurring in the mode MUX and DEMUX.

The crosstalk and coupling estimated from the measured channel impulse response in Fig. 3 are listed in table I. The coupling in the fiber is found to be more than 10 dB lower than the crosstalk in the mode MUX/DEMUX. Therefore, the channel impulse response shows a sparse characteristic. We can also see that the strongest crosstalk occurs when launching the LP01 mode and receiving the LP11b mode. This also agrees with the mode transfer matrix as shown in Fig. 2 (b). However, there is a mismatch of the crosstalk levels shown in Fig. 2, obtained by launching a single mode, and the measured impulse response shown in table I. We attribute this to the fact that the non-diagonal elements in table I are a combination of the effects arising from the aberrations caused by using both the central and offset SMFs in the fiber arrays of the MUX/DEMUX, as well as

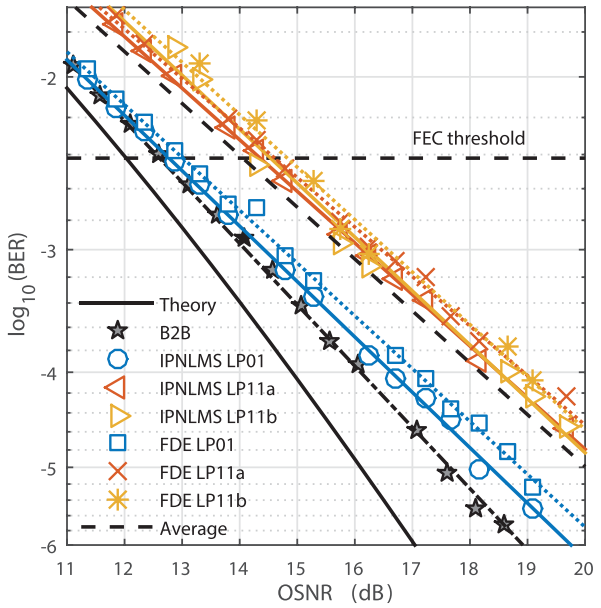

Fig. 4. BER versus OSNR for the IPNLMS and the conventional LMS FDE.

the superposition of phase masks for each channel in the transmission experiment.

B. System Performance

In order to mitigate the crosstalk, an equalizer with the same length as the channel impulse response is required, which is a length of 512 taps, so that it compensates the impulses due to the crosstalk between the three fiber modes as shown in Fig. 3. The number of equalizer taps is chosen to be a power of 2 for the increased efficiency of the fast Fourier transforms (FFTs) that are used in the FDE.

In order to reduce the additional noise introduced by the inactive taps in the conventional FDE, an adaptive sparse FDE using the IPNLMS algorithm is employed. In this equalizer, the taps with higher magnitudes are updated with a larger weight than those with lower magnitudes. Hence, the inactive taps remain suppressed close to their initial values, which are set to zero at the start of the equalization [11]. The measured BERs as a function of the received OSNRs are plotted in Fig. 4. The penalty from theory at the forward error correction (FEC) threshold is 0.4 dB for the LP01 mode and 1.8 dB for the LP11a/b modes. The required OSNR at the FEC threshold is reduced by approximately 0.2 dB by using the IPNLMS FDE (solid lines) comparing to the conventional FDE (dotted lines). The averaged BER of the three channels for back-to-back and after transmission is also plotted in Fig. 4, which indicates the average penalty induced by the mode multiplexing is approximately 1.46 dB. In Fig. 3, the impulses in the shaded areas represent the crosstalk between the selected modes and the other higher order modes at the MUX/DEMUX. The power of these impulses is higher in the observed channel response at the LP11a/b receivers (second and the third row) than in the LP01 receiver (first row). This indicates that there is more power coupled into the higher order modes from the LP11a/b modes than that from the LP01 mode at the mode MUX/DEMUX, which is also indicated in the mode transfer matrix in Fig. 2. This coupling of the LP11 modes to higher order modes has also been observed in MDM systems in the presence of non-ideal fiber connections [12]. Therefore, the LP11a/b modes incur an additional penalty due to the power that is coupled into the higher order modes and not received or processed by the MIMO equalizer.

IV. Conclusion

The transmission of three LP modes over an 8 km conventional GI-MMF is achieved using a compact SLM-based MUX and DEMUX. The SLMs display superposition of phase masks calculated to map LP modes of the fiber to different ports of an SMF array. An OSNR penalty of 0.4 dB and 1.8 dB from theory is found for the LP01 mode and LP11a/b modes respectively. Employing a sparse FDE updated with the IPNLMS algorithm to overcome the crosstalk induced by the MUX/DEMUX improves the system performance by 0.2 dB over the conventional FDE. However, the LP11a/b modes suffer an extra penalty of 1.4 dB compared to the LP01 mode as a result of coupling power into higher order modes at the MUX/DEMUX which is not processed by the MIMO receiver in this experiment.

Acknowledgment

The authors would like to thank Corning Inc. for supplying the fiber.

References

[1] M. A. Taubenblatt, "Space division multiplexing in data communications and high performance computing," in *Proc. IEEE Photon. Soc. Summer Topical Meeting Ser.*, Jul. 2012, pp. 195–196.

[2] M.-J. Li, "MMF for high data rate and short length applications," in *Proc. Opt. Fiber Commun. Conf. (OSA)*, Mar. 2014, pp. 1–3, paper M3F.1.

[3] S. Randel *et al.*, "Mode-multiplexed 6 × 20-GBd QPSK transmission over 1200-km DGD-compensated few-mode fiber," in *Proc. Opt. Fiber Commun. Conf. (OFC)*, Mar. 2012, pp. 1–3, paper PDP5C.5.

[4] E. Ip *et al.*, "146λ × 6 × 19-Gbaud wavelength- and mode-division multiplexed transmission over 10 × 50-km spans of few-mode fiber with a gain-equalized few-mode EDFA," *J. Lightw. Technol.*, vol. 32, no. 4, pp. 790–797, Feb. 15, 2014.

[5] V. A. Sleiffer *et al.*, "Field demonstration of mode-division multiplexing upgrade scenarios on commercial networks," *Opt. Exp.*, vol. 21, no. 25, p. 31036, Dec. 2013.

[6] R. Ryf *et al.*, "Mode-multiplexed transmission over conventional graded-index multimode fibers," *Opt. Exp.*, vol. 23, no. 1, pp. 235–246, Jan. 2015.

[7] M. Salsi, C. Koebele, G. Charlet, and S. Bigo, "Mode division multiplexed transmission with a weakly-coupled few-mode fiber," in *Proc. Opt. Fiber Commun. Conf. (OFC)*, Mar. 2012, pp. 1–3, paper OTu2C.5.

[8] M. Salsi *et al.*, "Mode-division multiplexing of 2×100 Gb/s channels using an LCOS-based spatial modulator," *J. Lightw. Technol.*, vol. 30, no. 4, pp. 618–623, Feb. 15, 2012.

[9] J. Carpenter, B. C. Thomsen, and T. D. Wilkinson, "Degenerate mode-group division multiplexing," *J. Lightw. Technol.*, vol. 30, no. 24, pp. 3946–3952, Dec. 15, 2012.

[10] K. Shi, G. Gordon, M. Paskov, J. Carpenter, T. D. Wilkinson, and B. C. Thomsen, "Degenerate mode-group division multiplexing using MIMO digital signal processing," in *Proc. IEEE Photon. Soc. Summer Topical Meeting Ser.*, Jul. 2013, pp. 141–142.

[11] K. Shi and B. C. Thomsen, "Sparse adaptive frequency domain equalizers for mode-group division multiplexing," *J. Lightw. Technol.*, vol. 33, no. 2, pp. 311–317, Jan. 15, 2015.

[12] J. Vuong *et al.*, "Mode coupling at connectors in mode-division multiplexed transmission over few-mode fiber," *Opt. Exp.*, vol. 23, no. 2, pp. 1438–1455, Jan. 2015.